

NONLINEAR OPTICS https://doi.org/10.1070/QEL18012

Ultra-broadband mid-infrared frequency combs produced by optical subharmonic generation

K.L. Vodopyanov

Abstract. **Optical frequency combs have revolutionised accurate frequency and time measurements and have enabled broadband and simultaneously high resolution spectroscopic measurements that were not previously possible. This paper is an overview of the main results of the previously performed work, describing a new approach to extending frequency combs to the mid-infrared 'molecular signature' range using a subharmonic generator based on an optical parametric oscillator operating in degenerate mode. Such an instrument acts as an efficient frequency divider that rigorously down-converts and augments the spectrum of a pump laser frequency comb while maintaining its coherence. Our recent result is the demonstration of a subharmonic system with a two-octave spectrum, 3–12 μm, which covers vibrational resonances for most molecular species. Potentially, through frequency division in the coherent subharmonic optical parametric amplifier regime, this method can be used to obtain intense long-wavelength pulses for high-field physics applications.**

Keywords: *frequency comb, optical subharmonic generation, mid-infrared range, degenerate optical generation.*

1. Introduction

Optical frequency combs – manifolds of evenly spaced and phase-locked narrow spectral lines produced by phase-stabilised femtosecond lasers – were introduced in the late 1990s and have revolutionised accurate measurements of frequency and time [1], culminating in the 2005 Nobel Prize in Physics. Subsequently, it has been shown that in spectroscopic applications, frequency combs can provide unprecedented spectral resolution surpassing narrow-linewidth tunable lasers [2]. The development of the idea of 'measuring the frequency of light with mode-locked lasers' would not have been possible without the fundamental contribution of the teams led by Veniamin Chebotaev (Novosibirsk) [3, 4], Theodor Hänsch (Munich) [5] and John Hall (Boulder, Colorado) [6].

Frequency combs are typically produced by stabilised femtosecond lasers and are characterised by a broad spectrum consisting of evenly spaced, phase-coherent narrow spectral lines with the spectral width that can be less than 1 Hz. The output of a mode locked laser can be viewed as a frequency comb provided that the laser repetition rate, f_{rep}, and the comb offset from zero – the carrier-envelope offset frequency, $f_{CEO,}$ – are both stabilised to a high degree of accuracy. Achieving frequency combs in the highly desirable mid-infrared ($\lambda > 3$ μm) range is a challenging task since direct broadband comb sources from mode locked lasers, similar to Ti:sapphire or Yb/Er-fibre lasers in the near infrared, are nonexistent [7, 8]. Below an overview is presented of our previous work on the creation of ultra-broadband mid-infrared (MIR) frequency combs.

K.L. Vodopyanov College of Optics and Photonics (CREOL), University of Central Florida, Orlando, Florida 32816, USA;
e-mail: vodopyanov@creol.ucf.edu

Received 2 February 2022
Kvantovaya Elektronika **52** (4) 307–312 (2022)
Submitted in English

2. Optical subharmonic oscillator

Resonant systems with parametric excitation that show subharmonic response are known in acoustics and mechanics since the 19th century. Faraday observed that the standing waves on liquid surfaces oscillated with one-half the frequency of the applied vertical periodic acceleration [9]. Later, subharmonic parametric oscillators were explored in the microwave [10] and, after the discovery of the possibility of optical parametric amplification [11], in the optical domain [12]. The main feature of these devices is that the subharmonic oscillation is phase locked to the driving force.

In an optical parametric oscillator (OPO) pumped by a laser at a cycle frequency ν_p, the photon energy conservation dictates that $\nu_p = \nu_s + \nu_i$, where ν_s and ν_i are the OPO signal and idler frequencies. Assuming that electric fields of the pump, signal, and idler are correspondingly in the form $E_p\cos(2\pi\nu_p t + \varphi_p)$, $E_s\cos(2\pi\nu_s t + \varphi_s)$, and $E_i\cos(2\pi\nu_i t + \varphi_i)$, the relationship between their phases is expressed as:

$$\varphi_p = \varphi_s + \varphi_i + \frac{\pi}{2} + \text{integer} \times 2\pi\,, \tag{1}$$

which ensures that the energy flows from the pump to the signal and idler waves [13]. The signal and idler phases φ_s and φ_i, however, are free to adopt any value as long as Eqn (1) is satisfied. In a degenerate divide-by-2 OPO, this degree of freedom disappears when the (co-polarised) signal and idler become indistinguishable, which leads to $\varphi_s = \varphi_i$. Hence, (1) becomes

$$\varphi_p = 2\varphi_{s,i} + \frac{\pi}{2} + \text{integer} \times 2\pi\,, \tag{2}$$

and phase coherence between the OPO and the pump is established. Also, when the subharmonic changes its phase by π (flips sign), the total phase difference changes by 2π and (2) still remains valid. This corresponds to the two possible phase states, called '0' and 'π' states.

When synchronously pumped by a frequency comb, the pump and the subharmonic OPO outputs are represented by a manifold of longitudinal modes sharing the same mode spacing equal to the pump pulse repetition frequency f_{rep}. Figure 1 sketches the spectrum of a degenerate synchronously pumped OPO. Since both (signal and idler) are resonant, their spectral components need to overlap with the OPO cavity resonances. The pump frequency comb modes are expressed as

$$\nu_n = f_{CEO} + nf_{rep}, \tag{3}$$

where n is an integer centred around some large number $n_0 = 10^6 - 10^7$ and f_{CEO} is the carrier envelope offset frequency ($0 \leqslant f_{CEO} < f_{rep}$). From the requirement of the photon energy conservation, it follows that the OPO modes can be aligned in only two ways (scenarios A&B in Fig. 1), namely

$$\nu_{m\,A} = f_{CEO}/2 + mf_{rep} \tag{4}$$

or

$$\nu_{m\,B} = f_{CEO}/2 + (m + 1/2)f_{rep}. \tag{5}$$

The choice between scenarios A&B is deterministically chosen by adjusting cavity resonances via changing the OPO cavity length with a piezoactuator. The time domain representation of the pump, as well as subharmonic states '0' and 'π', is shown in Fig. 2.

A schematic of a typical subharmonic OPO system is presented in Fig. 3. Massive cross mixing within the manifold of comb lines not only provides phase and frequency locking of the mid-IR comb lines to the pump, but also results in enhanced bandwidth (in frequency units) relative to the pump. Salient features of our approach include: (i) simplicity of the setup, (ii) low (<100 mW) pump power requirement with the threshold typically below 10 mW, (iii) potential for high (>50%) conversion efficiency, and (vi) possibility of achieving more-than-octave-wide spectrum due to the wide acceptance bandwidth of the nonlinear gain contour near degeneracy.

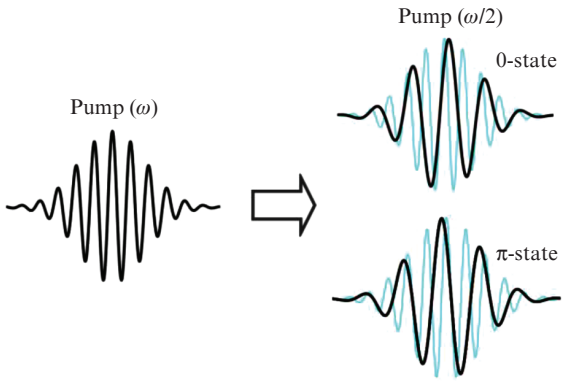

Figure 2. (Colour online) Time domain representation for electric field waveforms of pump and subharmonic pulses. Two possible phase states, '0' and 'π', are generated randomly in the subharmonic oscillator, based on a quantum noise seed.

Subharmonic OPOs pumped by near-infrared femtosecond lasers have allowed extending broadband comb sources to the MIR range [13, 14] and are now widely used in spectroscopic studies [15]. A subharmonic OPO is a coherent frequency divider that rigorously both down converts and augments the spectrum of the pump laser [16] without any excess phase noise [17]. Its main benefits are low oscillation threshold, broad bandwidth, and excellent stability when actively locked in operation at subharmonic. Yet another advantage is high conversion efficiency from the pump laser (64% was achieved in [18]) and high output power (close to 0.5 W was achieved in [19] at 1-GHz repetition rate and 3–8 μm instantaneous wavelength span).

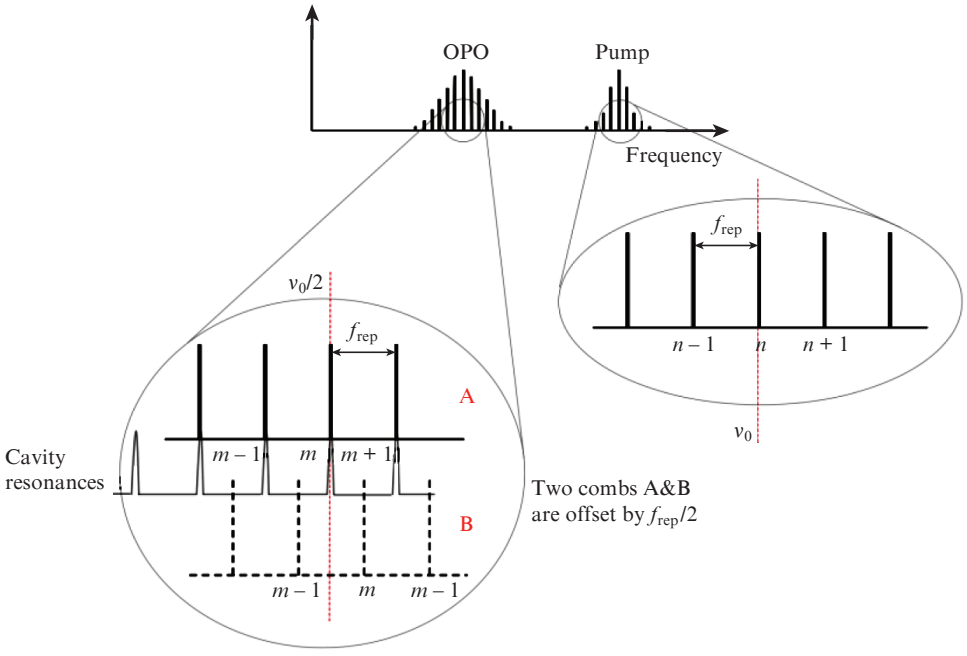

Figure 1. (Colour online) Frequency domain representation of pump laser and subharmonic OPO modes.

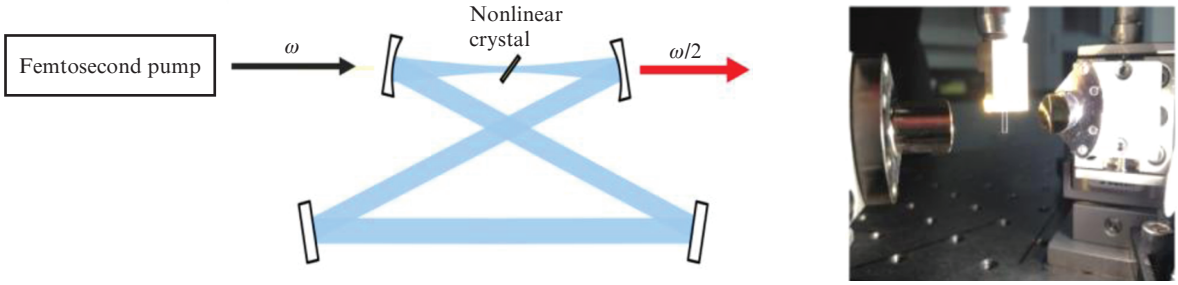

Figure 3. (Colour online) Schematic of a typical subharmonic OPO system. The inset shows a nonlinear gain crystal, namely 0.5-mm-thick periodically poled lithium niobate at Brewster's angle enclosed between the two off-axis parabolic mirrors.

Table 1. Subharmonic frequency combs achieved with a variety of pump lasers and nonlinear crystals.

Femtosecond pump laser	Nonlinear crystal	Instantaneous spectral span/μm	Refs
Er-fibre at 1560 nm	Periodically poled $LiNbO_3$, 200–500-μm long	2.5–3.8	[13]
Er-fibre at 1560 nm	Orientation-patterned GaP, 500-μm long	2.3–4.8	[20]
Cr:ZnSe at 2425 nm	Orientation-patterned GaAs, 500-μm long	4.4–5.4	[21]
Tm-fibre at 2050 nm	Orientation-patterned GaAs, 500-μm long	2.6–6.1	[22]
Cr:ZnS at 2380 nm	Orientation-patterned GaAs, 500-μm long	3.6–5.6	[23]
Tm-fibre at 1930 nm	Orientation-patterned GaAs, 500-μm long	2.6–7.5	[16]
Cr:ZnS at 2350 nm	Orientation-patterned GaAs, 500-μm long	2.85–8.4	[24]
Cr:ZnS at 2350 nm	Polycrystalline ZnSe, 1.5-mm-long	3–7	[25]
Cr:ZnS at 2350 nm	Orientation-patterned GaP, 500-μm long	3–12	[26]

Table 1 summarises subharmonic frequency combs achieved in our group with a variety of femtosecond pump lasers and nonlinear crystals.

3. Dual comb spectroscopy

There are several scenarios where frequency combs can be used for spectroscopy [27]: (i) a broadband comb directly interrogates an absorbing sample after which the spectrum is dispersed in two dimensions and sensed with a 2D detector array [28, 29], (ii) a frequency comb is used as a light source in Michelson-interferometer-based Fourier-transform spectroscopy [30–33], and (iii) dual-comb spectroscopy [34, 35].

Dual comb spectroscopy (DCS) is currently the most advanced spectroscopic technique in the MIR range. Here, the second frequency comb, with a small offset of the mode spacing (same as f_{rep}) with respect to the first comb, effectively plays the role of the Doppler-shifted second arm in the Michelson interferometer. The price to pay, however, is that DCS technique requires a high degree of mutual coherence between the two combs. With our new approach to producing MIR combs, we implemented a DCS system that used a pair of subharmonic OPOs pumped by a pair of phase-locked Tm-fibre frequency combs [15]. The system provided fast, up to 150 spectra per second, moving-parts-free, simultaneous acquisition of 350000 spectral data points, spaced by a 115 MHz (comb-line spacing) over the whole wavelength range of 3.1–5.5 μm and provided massively parallel trace molecular sensing in a mixture of ten gases (OCS, N_2O, NO, CO, CH_4, C_2H_6, C_2H_4, C_2H_2, CO_2, and H_2O) and their isotopologues at part-per-million-level concentrations. Figure 4 shows the DCS setup and illustrates spectroscopic detection

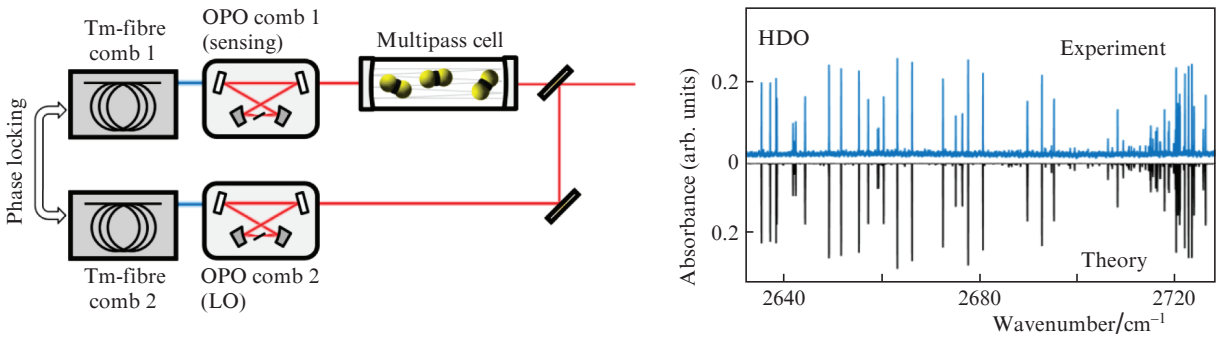

Figure 4. (Colour online) Dual-frequency-comb setup and the absorption spectrum of water isotopologue containing deuterium (HDO) measure in ambient air.

of water isotopologue containing deuterium (HDO) just in ambient room air.

4. Subharmonic oscillator with two-octave wide instantaneous spectrum

Our latest result on broadband comb generation in the MIR is a subharmonic comb with an ultra-broadband instantaneous spectrum spanning 3–12 μm [26]. The key to getting such a broad spectrum was the use of a long-wavelength femtosecond pump laser – a Kerr-lens mode-locked Cr:ZnS oscillator with 2.35 μm centre wavelength, 79 MHz repetition frequency, and bandwidth-limited pulse duration of 62 fs. The progress in the development of mode-locked Cr:ZnS/Cr:ZnSe lasers [36, 37] became possible thanks to the efforts of the team of Evgeni Sorokin and Irina Sorokina and the team of Sergey Mirov (they all got their Candidate of Sciences degrees from the Prokhorov General Physics Institute, Moscow). Most recently, Mirov's group has demonstrated the first super-octave (1.6–3.2 μm) long-wavelength ultrafast laser based on a Kerr-lens mode-locked Cr:ZnS oscillator [38].

Yet another key to achieve a broad spectrum from our subharmonic OPO was a minimally dispersive cavity that used (i) all gold-coated mirrors, (ii) a special 'injector' mirror for letting the pump radiation in, and (iii) optically thin intracavity elements with zero group velocity dispersion crossings near the OPO spectral midpoint. At the average 2.35-μm pump power of 1.2 W, the OPO delivered 245 mW of the output power with the conversion efficiency exceeding 20%. A broad bandwidth parametric gain was provided by a 0.5-mm-long orientation-patterned gallium phosphide (OP-GaP) – a

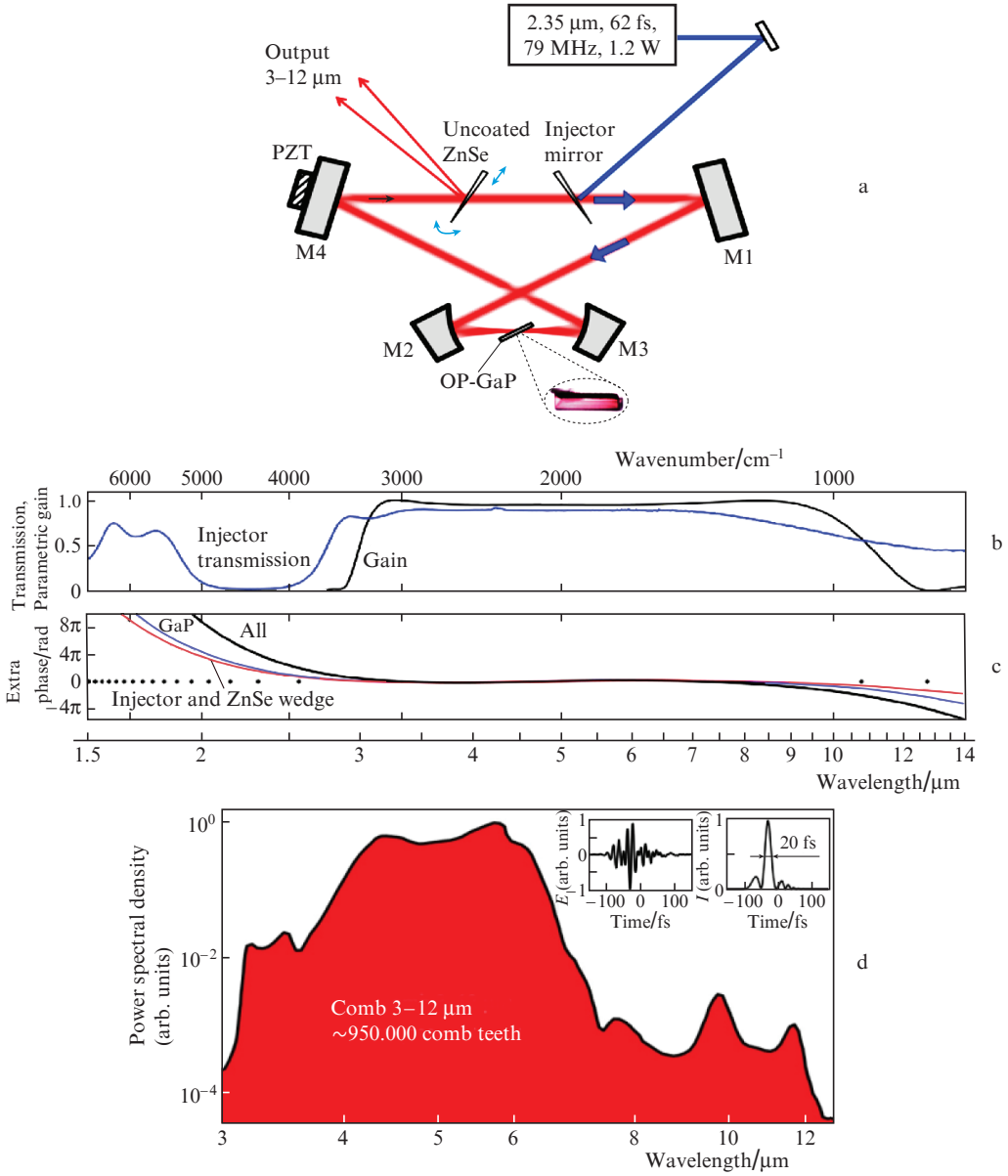

Figure 5. (a) Schematic of the 2.35-μm pumped subharmonic OPO (M1–M4, gold coated mirrors; PZT, piezoelectric transducer), (b) normalised parametric gain and injector transmission vs. wavelength (both wavelength and frequency are on a log scale), (c) extra phase per cavity round trip (black curve) and contribution of separate elements: OP-GaP (blue) and injector plus tuning wedge combined (red), and (d) the OPO output spectrum. The insets in (d) show simulated *E*-field and intensity *I* waveforms for the OPO pulses.

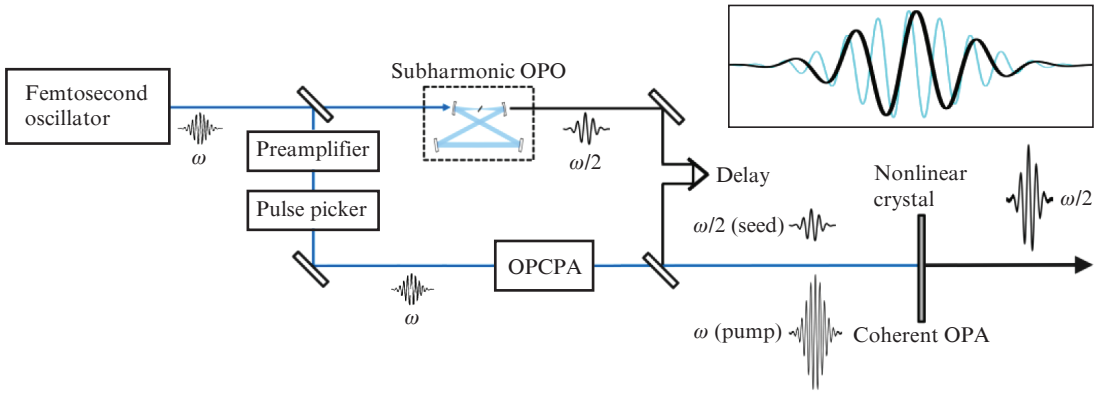

Figure 6. (Colour online) Schematic of the coherent subharmonic optical parametric amplifier for producing super-intense long-wavelenght MIR pulses. The seed pulse ($\omega/2$) is produced by a subharmonic OPO and is coherent to the pump (ω). The inset shows the relative position (relative phase) of the seed and the pump waveforms in the time domain.

quasi-phase-matched (QPM) crystal with wide transparency range of 0.55–13 μm and a large second-order nonlinear coefficient (d_{14} = 35 pm V^{-1}). The crystal had a QPM period of 110 μm and was placed at Brewster's angle with all the interacting waves co-polarised along ⟨111⟩ direction of GaP [26]. A typical OPO pump depletion in our experiments was as high as 83%. Figure 5 shows the OPO schematic, the wavelength dependence of the normalised parametric gain, the injector transmission, and an extra phase accumulated per cavity round trip for different intracavity elements, and the OPO output spectrum. This ultra-broadband MIR comb will be used in our next generation DCS setup, where two mutually coherent Cr:ZnS laser frequencies will pump two subharmonic OP-GaP OPOs.

5. Coherent subharmonic optical parametric amplifier

Many applications such as attosecond [39] and high-field physics [40], high-harmonic generation in gases [41] and solids [42, 43], and laser-driven plasma-based electron accelerators [44] require intense (~1 GW peak power) to super-intense (100 GW to 1 TW) pulses in the MIR. In all of these applications, long-wavelength (>5 μm) ultrafast pulses are most desirable.

The subharmonic generation method offers an efficient and elegant way of converting super-intense pulses obtained through OPCPA at some 'convenient' wavelengths, for example 2.4 μm or 4 μm, to half their frequency with high efficiency. A schematic of this proposed approach is shown in Fig. 6. Part of the femtosecond frequency comb laser output (at frequency ω) serves as a pump for the subharmonic OPO and generates an output at frequency $\omega/2$, which serves as a seed for a coherent optical parametric amplifier (OPA). The main part of the laser output is amplified in a preamplifier and, after picking a single pulse, in an OPCPA up to a high (from 10 to 100 mJ) pulse energy. Next, the subharmonic seed pulse at $\omega/2$ is overlapped with the intense amplified pulse at ω and is converted into a subharmonic at $\omega/2$. A very high conversion efficiency (50%–90%) is expected due to the fact that all photons are recycled in this scheme. One of the important features of a coherent OPA is that the seed at $\omega/2$ and the pump pulse at ω must be (in contrast to traditional OPAs) mutually coherent. This is achieved automatically, since the $\omega/2$ pulse is phase locked to the ω pulse. The relative phase (relative delay) between the two in the coherent subharmonic OPA must be adjusted with sub-wavelength accuracy (few 10 nm) according to Eqn (2). This may be achieved using a piezoactuator. The inset in Fig. 6 shows the relative position in the time domain of $\omega/2$ and ω pulses.

6. Conclusion

Subharmonic generation, which can be viewed as second harmonic generation inverted, is an effective way to extend the wavelength range of well-developed near-IR frequency combs to the MIR region. The main advantages are high conversion efficiency, intrinsic phase and frequency locking to the near-IR pump comb, and the bandwidth that can be much broader than that of the pump frequency comb. The best result to date is a broadband, 3–12 μm, subharmonic OPO that can be used for massively parallel molecular detection using DCS. Another interesting possibility (not yet realised) is a coherent subharmonic OPA for converting intense laser pulses to half their centre frequency to produce long-wavelength MIR pulses that are highly desirable for high-field physics.

References

1. Udem T., Holzwarth R., Hänsch T.W. *Nature*, **416**, 233 (2002).
2. Gatti D., Sala T., Marangoni M., Galzerano G., Gianfrani L., in *Encyclopedia of Analytical Chemistry: Applications, Theory and Instrumentation* (New York: Wiley, 2011).
3. Baklanov E.V., Chebotaev V.P. *Sov. J. Quantum Electron.*, **7**, 1252 (1977) [*Kvantovaya Elektron.*, **4**, 2189 (1977)].
4. Letokhov V.S., Chebotaev V.P. *Springer Series in Optical Sciences* (New York: Springer, 1977).
5. Hänsch T.W. *Rev. Mod. Phys.*, **78**, 1297 (2006).
6. Hall J.L. *Rev. Mod. Phys.*, **78**, 1279 (2006).
7. Schliesser A., Picqué N., Hänsch T.W. *Nature Photon.*, **6**, 440 (2012).
8. Vodopyanov K.L. *Laser-based Mid-infrared Sources and Applications* (New York: Wiley, 2020).
9. Faraday M. *Philos. Trans. R. Soc. Lond.*, **121**, 319 (1831).
10. Louisell W.H. *Coupled Mode and Parametric Electronics* (New York: Wiley, 1960).
11. Akhmanov S., Kovrigin A., Piskarskas A., Fadeev V., Khokhlov R. *JETP Lett.*, **2**, 191 (1965) [*Pis'ma Zh. Eksp. Teor. Fiz.*, **2**, 300 (1965)].
12. Nabors C.D., Yang S.T., Day T., Byer R.L. *J. Opt. Soc. Am. B*, **7** (5), 815 (1990).
13. Wong S.T., Vodopyanov K.L., Byer R.L. *J. Opt. Soc. Am. B*, **27**, 876 (2010).

14. Leindecker N., Marandi A., Byer R.L., Vodopyanov K.L. *Opt. Express*, **19**, 6296 (2011).
15. Muraviev A.V., Smolski V.O., Loparo Z.E., Vodopyanov K.L. *Nat. Photonics*, **12**, 209 (2018).
16. Smolski V.O., Yang H., Gorelov S.D., Schunemann P.G., Vodopyanov K.L. *Opt. Lett*., **41**, 1388 (2016).
17. Wan C., Li P., Ruehl A., Hartl I. *Opt. Lett*., **43**, 1059 (2018).
18. Marandi A., Ingold K.A., Jankowski M., Byer R.L. *Optica*, **3**, 324 (2016).
19. Smolski V., Vasilyev S., Moskalev I., Mirov M., Ru Q., Muraviev A., Schunemann P., Mirov S., Gapontsev V., Vodopyanov K. *Appl. Phys. B*, **124**, 101 (2018).
20. Ru Q., Loparo Z.E., Zhang X., Crystal S., Vasu S., Schunemann P.G., Vodopyanov K.L. *Opt. Lett*., **42**, 4756 (2017).
21. Vodopyanov K.L., Sorokin E., Sorokina I.T., Schunemann P.G. *Opt. Lett*., **36**, 2275 (2011).
22. Leindecker N., Marandi A., Byer R.L., Vodopyanov K.L., Jiang J., Hartl I., Fermann M., Schunemann P.G. *Opt. Express*, **20**, 7047 (2012).
23. Smolski V.O., Vasilyev S., Schunemann P.G., Mirov S.B., Vodopyanov K.L. *Opt. Lett*., **40**, 2906 (2015).
24. Ru Q., Zhong K., Lee N.P., Loparo Z.E., Schunemann P.G., Vasilyev S., Mirov S.B., Vodopyanov K.L., in *Techn. Digest Conf. on Lasers and Electro-Optics* (OSA, 2017) paper SM4M.3.
25. Ru Q., Lee N., Chen X., Zhong K., Tsoy G., Mirov M., Vasilyev S., Mirov S.B., Vodopyanov K.L. *Optica*, **4**, 617 (2017).
26. Ru Q., Kawamori T., Schunemann P.G., Vasilyev S., Mirov S.B., Vodopyanov K.L. *Opt. Lett*., **46**, 709 (2021).
27. Picqué N., Hänsch T.W. *Nat. Photonics*, **13**, 146 (2019).
28. Diddams S.A., Hollberg L., Mbele V. *Nature*, **445**, 627 (2007).
29. Nugent-Glandorf L., Neely T., Adler F., Fleisher A.J., Cossel K.C., Bjork B., Dinneen T., Ye J., Diddams S.A. *Opt. Lett*., **37**, 3285 (2012).
30. Foltynowicz A., Maslowski P., Ban T., Adler F., Cossel K.C., Briles T.C., Ye J. *Faraday Discuss*., **150**, 23 (2011).
31. Haakestad M.W., Lamour T.P., Leindecker N., Marandi A., Vodopyanov K.L. *J. Opt. Soc. Am. B*, **30**, 631 (2013).
32. Meek S.A., Poisson A., Guelachvili G., Hänsch T.W., Picqué N. *Appl. Phys. B*, **114** (4), 573 (2014).
33. Khodabakhsh A., Ramaiah-Badarla V., Rutkowski L., Johansson A.C., Lee K.F., Jiang J., Mohr C., Fermann M.E., Foltynowicz A. *Opt. Lett*., **41**, 2541 (2016).
34. Keilmann F., Gohle C., Holzwarth R. *Opt. Lett*., **29**, 1542 (2004).
35. Schliesser A., Brehm M., Keilmann F., van der Weide D.W. *Opt. Express*, **13**, 9029 (2005).
36. Sorokina I.T. *Opt. Mater.*, **26**, 395 (2004).
37. Mirov S., Fedorov V., Martyshkin D., Moskalev I., Mirov M., Vasilyev S. *IEEE J. Sel. Top. Quantum Electron*., **21**, 1601719 (2015).
38. Vasilyev S., Moskalev I., Smolski V., Peppers J., Mirov M., Barnakov Y., Fedorov V., Martyshkin D., Mirov S., Gapontsev V. *Opt. Express*, **29**, 2458 (2021).
39. Corkum P.B., Krausz F. *Nat. Phys*., **3**, 381 (2007).
40. Shcherbakov M.R., Zhang H., Tripepi M., Sartorello G., Talisa N., Al-Shafey A., Fan Z., Twardowski J., Krivitsky L.A., Kuznetsov A.I., Chowdhury E., Shvets G. *Nat. Commun*., **12**, 4185 (2021).
41. Popmintchev T., Chen M-C., Arpin P., Murnane M.M., Kapteyn H.C. *Nat. Photonics*, **4**, 822 (2010).
42. Ghimire S., Reis D.A. *Nat. Phys*., **15**, 10 (2019).
43. Shcherbakov M.R., Zhang H., Tripepi M., Sartorello G., Talisa N., AlShafey A., Fan Z., Twardowski J., Krivitsky L.A., Kuznetsov A.I., Chowdhury E., Shvets G. *Nat. Commun*., **12**, 4185 (2021).
44. Esare E., Schroeder C.B., Leemans W.P. *Rev. Modern Phys*., **81**, 1229 (2009).